

## UDCA-LPE Inhibits Lipoapoptosis by Shifting Fatty Acid Pools towards Mono- and Polyunsaturated Fatty Acids in Mouse Hepatocytes

Walee Chamulitrat, Gerhard Liebisch, Weihong Xu, Hongying Gan-Schreier, Anita Pathil, Gerd Schmitz, Wolfgang Stremmel

Department of Internal Medicine IV, Gastroenterology and Infectious Diseases, Im Neuenheimer Feld 410, 69120 Heidelberg, Germany (W.C., H.G.-S., A.P., W.S); Institute of Clinical Chemistry and Laboratory Medicine, University of Regensburg, Franz-Josef-Strauss-Allee 11, 93053 Regensburg, Germany (G.L., G.S); and Department of Gastroenterology, Hangzhou the first people's hospital, Hangzhou, Zhejiang, P.R. China (W.X.)

Running title: Lipoprotection by UDCA-LPE

Corresponding author: Walee Chamulitrat, Internal Medicine IV, Im Neuenheimer Feld 345 EG,  
69120 Heidelberg, Germany. Tel: 049-6221-56-38731; Fax: 049-6221-56-5398; email:

Walee.Chamulitrat@med.uni-heidelberg.de.

35 Text pages

3 Tables

1 Supplemental Table

6 Figures

50 References

218 words in Abstract

599 words in Introduction

1156 words in Discussion

Abbreviations:

AA, arachidonic acid; ACC1, acetyl-CoA carboxylase; Acox1, acyl-CoA oxidase 1; ATGL, adipocyte triglyceride lipase ;cAMP, cyclic adenosine monophosphate; CDCA, chenodeoxycholic acid; CPT-2-Me-cAMP, 8-(4-chlorophenylthio)-2'-O-methyladenosine 3',5'-cyclic monophosphate; DGAT1 and DGAT 2, diacylglycerol acyltransferase 1 and 2; DHA, docosahexaenoate; DPA, docosapentaenoate; Elovl, fatty acid elongase; EPAC, exchange protein activated by cAMP; ESI-MS/MS, electrospray ionization tandem mass spectrometry; Fads, fatty acid desaturase; FAS, fatty acid synthase; GC-MS, gas chromatography coupled to mass spectrometry; GPCR, G-protein coupled receptor; LPE, 18:1n9-lysophosphatidylethanolamine; LXR, liver X receptor; MUFA, monounsaturated fatty acids; NASH, non-alcoholic steatohepatitis; Pal, pamate; PARP-1, poly ADP-ribose polymerase-1; PC, phosphatidylcholine; PE, phosphatidylethanolamine; PI, phosphatidylinositol; PKA, protein kinase A; PPAR, peroxisome proliferator-activated receptor activators; PS, phosphatidylserine; PUFA, polyunsaturated fatty acids; SCD-1, stearoyl-CoA desaturase-1; SFA, saturated fatty acids; SREBP1, sterol regulatory element-binding protein1;TG, triglycerides; UDCA, ursodeoxycholic acid; UDCA-LPE, ursodeoxycholyl lysophosphatidylethanolamide

## ABSTRACT

Ursodeoxycholyly lysophosphatidylethanolamide (UDCA-LPE) is hepatoprotectant in inhibiting apoptosis, inflammation, and hyperlipidemia in mouse models of non-alcoholic steatohepatitis (NASH). We herein studied the ability of UDCA-LPE to inhibit palmitate (Pal)-induced apoptosis in primary hepatocytes, and delineate cytoprotective mechanisms. We showed that lipoprotection by UDCA-LPE was mediated by adenosine 3', 5'-cyclic monophosphate (cAMP), and was associated with increases of triglycerides (TG) and phospholipids (PL). An inhibitor of cAMP-effector protein kinase A partially reversed protective effects of UDCA-LPE. Lipidomic analyses of fatty acids and PL composition revealed a shift of lipid metabolism from saturated Pal to mono- and polyunsaturated fatty acids, mainly, oleate, docosapentaenoate and docosahexaenoate. The latter two  $\omega$ -3 fatty acids were particularly found in phosphatidylcholine and phosphatidylserine pools. The catalysis of Pal by stearoyl-CoA desaturase-1 (SCD-1) is a known mechanism for the channelling of Pal away from apoptosis. SCD-1 protein was upregulated during UDCA-LPE lipoprotection. SCD-1 knockdown of Pal-treated cells showed further increased apoptosis and the extent of UDCA-LPE protection was reduced. Thus, the major mechanism of UDCA-LPE lipoprotection involved a metabolic shift from toxic saturated towards cytoprotective unsaturated fatty acids in part via SCD-1. UDCA-LPE may thus be a therapeutic agent for treatment of NASH by altering distinct pools of fatty acids for storage into TG and PL, and the latter may protect lipotoxicity at the membrane levels.

## Introduction

Non-alcoholic steatohepatitis (NASH) is the most common form of chronic liver disease and is associated with metabolic syndrome and obesity (Diehl, 1999). NASH is defined as lipid accumulation with cellular damage, inflammation and different degree of fibrosis. NASH is considered a serious condition as 25% of these patients can progress to cirrhosis, portal hypertension, and the condition with a high risk of hepatocellular carcinoma. Numerous advances in understanding its pathogenesis have been made providing a rationale for translation into clinical trials. Besides dietary modification and bariatric surgery, pharmacological interventions have been tested including insulin sensitizers, peroxisome proliferator activated nuclear receptor- $\gamma$  agonists, TNF- $\alpha$  antagonists, lipid-lowering agents as well as antioxidants and hepatoprotectants (Satapathy, and Sanyal, 2010). Clinical trials using insulin sensitizers such as metformin and glitazones have revealed ineffectiveness or only partial efficacy (Ratziu et al., 2010). Histological improvement of disease, at least in some patients, is observed with vitamin E (Satapathy and Sanyal, 2010) and ursodeoxycholic acid (UDCA) (Ratziu et al., 2011). UDCA at high-dose 28-35 mg/kg/day has been shown to improve aminotransferase levels, serum fibrosis markers, and selected metabolic parameters (Ratziu et al., 2011).

It is known that UDCA is a hepatoprotectant (Rodrigues et al., 1998), anti-inflammatory (Zhang et al., 2010) and antifibrotic agent (Zhang et al., 2010), and is approved for treatment of cholestatic liver disease (Tsochatzis et al., 2009). UDCA is efficiently taken up by bile acid transport proteins (Maeda et al., 2006), and the coupling of UDCA at C<sub>24</sub> with drugs, such as, 5-aminosalicylic acid (Goto et al., 2001) and cisplatin (Briz et al., 2002) renders efficient uptake by these transporters (Balakrishnan et al., 2006). Moreover, the C<sub>23</sub> homologue of UDCA, which lacks one methylene group in its side chain, so-called norUDCA, has been shown to be a better hepatoprotectant than UDCA in treatment of experimental sclerosing cholangitis (Fickert et al.,

2006) and NASH (Beraza et al., 2011). We had rationalized that efficacy of UDCA could be improved by a coupling of UDCA with a phospholipid because phospholipids are known to increase hepatocyte membrane integrity (Li et al., 2006). We performed a coupling at C<sub>24</sub> of UDCA with lysophosphatidylethanolamine (LPE; 18:1n-9-lysophosphatidylethanolamine) to generate ursodeoxycholyl lysophosphatidylethanolamide (UDCA-LPE) with a chemical structure shown in Fig. 1A (Chamulitrat et al., 2009). UDCA-LPE was shown to be cytoprotective as an intact compound. The superiority of UDCA-LPE to UDCA has been indeed demonstrated in terms of inhibition of TNF- $\alpha$ -induced apoptosis and protection against acute liver injury (Chamulitrat et al., 2009; Pathil et al., 2011). Furthermore, we have recently shown that UDCA-LPE administration of mice fed with high-fat diet could lower systemic and hepatic hyperlipidemia concomitant with significant inhibition of hepatocyte apoptosis and inflammation (Pathil et al., 2012).

The hallmark of NASH includes increases of hepatocellular saturated fatty acids and subsequent lipoapoptosis. In mouse hepatocytes, we herein demonstrated that UDCA-LPE could inhibit apoptosis induced by palmitate (Pal). We further investigated mechanisms of lipoprotection whether it could be mediated by cyclic adenosine monophosphate (cAMP) (Kwon et al., 2004), and by pathways associated with accumulation of triglycerides (TG) (Listenberger et al., 2003) and phospholipids (PL) (Collins et al., 2010). By using inhibitors and performing knockdown experiments, we showed that the latter was the major mechanism involving the action of stearoyl-CoA desaturase-1 (SCD-1), an enzyme which converts saturated-(SFA) to monosaturated fatty acids (MUFA). Lipidomic data revealed that UDCA-LPE was able to induce changes in fatty acid composition in lowering cytotoxic SFA and Pal while increasing MUFA and polyunsaturated fatty acids (PUFA) including docosapentaenoate (DPA) and docosahexaenoate (DHA). Thus, the major mechanism for UDCA-LPE lipoprotection *in vitro* appeared to involve alterations of fatty acid composition.

## Materials and Methods

**Reagents.** The synthesis of UDCA-LPE was reported previously (Chamulitrat et al., 2009). For UDCA-LPE used in this study, the same synthesis procedure was performed by ChemCon (Freiburg, Germany). Intracellular cyclic AMP was determined by ELISA kit (BT-730) from Hycultec GmbH, Beutelbach, Germany. Palmitate, BSA, neonatal calf serum, and N-TER<sup>TM</sup> Nanoparticle siRNA transfection system were obtained from Sigma (Taufkirchen, Germany). Brefeldin A and 8-(4-chlorophenylthio)-2'-O-methyladenosine 3',5'-cyclic monophosphate (8-CPT-2'-O-Me-cAMP) were obtained from Biomol, Hamburg, Germany. Adenosine 3',5'-cyclic monophosphate, N<sup>6</sup>,O<sup>2'</sup>-dibutyryl (dibutyryl-cAMP), adenosine 3',5'-cyclic monophosphate (8-bromo-cAMP), KT5720, and protease inhibitor cocktails were obtained from Calbiochem (Darmstadt, Germany). Sources of primary antibodies: SCD-1 (clone CD.E10) and Elovl6 (ab69857) were from Abcam (Cambridge, UK); cleaved PARP-1 (clone E51) was from Epitomics (Hamburg, Germany); Bim and cleaved caspase-3 (clone 5AIE) were from Cell Signaling Technologies (Frankfurt, Germany).

**Hepatocyte isolation.** Hepatocytes were isolated from 7-10 week old male C57/BL6 mice (Charles Rivers Laboratories, Sulzfeld, Germany) by using two-step collagenase perfusion technique and purified by Percoll. Freshly isolated hepatocytes were plated and cultured for 4 h in M199 medium containing Hank' salts and L-glutamine (PAA, Cölbe, Germany) supplemented with 1% penicillin and streptomycin, 100 nM dexamethasone, 0.5 nM insulin, and 4% neonatal calf serum. Dead hepatocytes were removed, and the adhered cells were treated with freshly prepared Pal with or without UDCA-LPE in serum-free M199 medium on the same day of isolation.

**Palmitate preparation and caspase 3 assay.** Pal stock solution in BSA was prepared according to published procedure (Rahman et al., 2009). Briefly, 250 µl of 200 mM Pal in ethanol was mixed with 4.5 ml of 27% BSA in PBS. The total 5 ml volume was adjusted to pH to 7.4 with 0.1 N NaOH until the mixture became clear. After treatment at indicated time, hepatocytes were washed with PBS and

lyzed with 1% Triton X-100 in PBS. Cell lysates after centrifugation were subjected to determination of protein (Bio-Rad<sup>DC</sup> Protein kit) and caspase 3/7 activity using Caspase 3/7<sup>Glo</sup> kit (Promega, Mannheim, Germany). Luminescence was measured with a Fluostars Optima (BMG Labtech GmbH, Germany). For solvent controls, wells without Pal contained 0.5% BSA and 0.1% ethanol.

**Immunoblotting.** After treatment, mouse hepatocytes plated in 6-well collagen coated plates were lysed and centrifuged at 13,000g, 4°C for 15 min. Cell lysates were separated by gel electrophoresis, and transferred onto PDVF membranes. Blots were treated with a primary antibody followed by a secondary antibody. Protein bands were visualized by using Luminata Forte ECL system (Millipore, Darmstadt, Germany).

**Lipid extraction, fatty acid and phospholipid analyses.** Lipid extraction of 100 µl lysates of treated mouse hepatocytes was performed according to Folch's method by using 10 volumes 2:1 chloroform:methanol. After removal of protein precipitates, chloroform was collected and evaporated to complete dryness. Lipids were dissolved in 50 µl 3:2 hexane:isopropanol. TG levels normalized to mg protein were determined with LabASSY Triglyceride kits (Wako GmbH, Germany) using a microplate reader Mutiskan Ascent (ThermoFisher Scientific, Germany). Treated mouse hepatocytes were taken up into 200 µl PBS and lysed by freeze-thawing. After centrifugation, lysates were subjected to fatty acid analyses by gas chromatography coupled to mass spectrometry (GC-MS) as previously described (Ecker et al., 2012) and quantification of phospholipids by electrospray ionization tandem mass spectrometry (ESI-MS/MS) in positive mode using the set-up described previously (Liebisch et al., 2004).

**Analyses of UDCA-LPE and UDCA.** Cell lysates were subjected to lipid extraction in the presence of D<sub>4</sub>-UDCA as an internal standard. UDCA-LPE and UDCA concentrations in samples and standards were determined using a liquid chromatography mass spectrometer (Waters 2695 interfaced with a Quattro Micro) (Chamulitrat et al., 2012).

**Gene expression by RT-PCR.** Total RNA of treated mouse hepatocytes was isolated using QIAGEN RNeasy Mini kit (Qiagen, Hilden, Germany). cDNA was synthesized from 2  $\mu$ g RNA using a Maxima First Strand cDNA synthesis kit (Fermentas, St. Leon-Rot, Germany). The mRNA expression was analyzed in quadruplets by real-time PCR using Applied Biosystems TaqMan® gene expression assays with TaqMan® Universal PCR Master Mix (Applied Biosystems) and run on an Applied Biosystem 7500 Fast real-time PCR machine by using assay-on-Demand TaqMan® primers. The expression level of targets in quadruplets was calculated using  $\Delta$ -C<sub>t</sub> transformation method, and determined as a ratio of target gene normalized to house-keeping gene GAPDH. PCR results were obtained from 3-4 independent experiments except for Fig. 5D showing representative results from 2 experiments.

**Small interfering RNA and transfection.** SCD-1 siRNAs were designed and synthesized by Riboxx GmbH, Radebeul, Germany. Two siRNA pairs were used in our study: SCD-1 siRNA\_1 (antisense: UUUACUAAAGA CACCAGGCCCCC and sense: GGGGGCCUGGUGU CUUUAAGU AAA); and SCD-1 siRNA\_2 (antisense: UAUUAGUACAUCAUCUGGCCCCC and sense GGGGGCCAG AUGAAUGUACUAAUA). Negative control siRNAs were obtained from Eurogentec (Seraing, Belgium). After allowing mouse primary hepatocytes to adhere for 4 h, cells were transfected with 50 nM con- or SCD-1- siRNAs using N-TER™ Nanoparticle siRNA transfection reagent for 4 h. Cells were subsequently treated with Pal with or without UDCA-LPE in serum-free M199 medium for further 9 or 20 h.

**Data analysis.** Results were expressed as mean  $\pm$  SD from at least two independent experiments performed at least in triplicates. For data in Figures, significance using ANOVA with Bonferroni's test for multiple comparisons was determined by using Graphpad Prism 5. For data in Tables, significance for multiple comparisons was computed using a call of the SAS procedure GLM for Tukey's and Bonferroni's tests. Dunnett's test was used for multiple testing against the control group.



## Results

### UDCA-LPE inhibits lipoapoptosis in part by cAMP/PKA signalling.

Treatment of mouse hepatocytes with 300  $\mu$ M Pal for 20 h induced significant apoptosis as evident by increased expression of pro-apoptotic BCl-2 family Bim, cleaved caspase 3 and cleaved poly-ADP-ribose polymerase-1 (PARP-1) proteins (Fig. 1B). Representative data from 3 experiments showed that co-treatment of Pal with 60  $\mu$ M UDCA-LPE significantly inhibited expression of pro-apoptotic proteins (Fig. 1B) and caspase 3 activities (Fig. 1C) by >90%. IC<sub>50</sub> for UDCA-LPE lipoprotection was determined to be ~32  $\mu$ M (Fig. 1D). An addition of UDCA-LPE 2 or 4 h post Pal addition decreased the extent of lipoprotection indicating that pre- and co-incubation was necessary for UDCA-LPE lipoprotection (Fig. 1E). Apoptosis inhibition was not observed upon co-treatment with 60  $\mu$ M UDCA, oleate (18:1n-9) or palmitoleate (16:1n-7) (Fig. 1F). Oleate or palmitoleate was found to be protective when used at 200  $\mu$ M (data not shown), which was in accordance with previous report (Listenberger et al., 2003; Collins et al., 2010). Co-treatment with LPE or individually added UDCA + LPE partially inhibited apoptosis by only ~25%. This is consistent with the reported anti-apoptotic activity of LPE with a mechanism of MAPK activation (Nishina et al., 2006). Pal co-treatment with other protective agents, *i.e.*, chenodeoxycholic acid (CDCA) (Pellicciari et al., 2004) or tauro-UDCA (Miller et al., 2007) at 60  $\mu$ M also did not elicit lipoprotection (Fig. 1G). This demonstrated the superiority of UDCA-LPE to some known cytoprotective lipids and bile acids.

It is known that cytoprotective bile acids can activate cAMP that mediates apoptosis protection against toxic bile acids (Webster et al., 1998). It is hypothesized that UDCA-LPE as a bile acid-PL conjugate may mediate protection against Pal toxicity via cAMP (Kwon et al., 2004). UDCA-LPE treatment of mouse hepatocytes for 30 min increased intracellular cAMP concentrations in a dose-dependent manner (Fig. 2A). Stimulation of cAMP by 100  $\mu$ M UDCA was

found to be lesser than that of UDCA-LPE. In a similar manner as UDCA-LPE, co-treatment of hepatocytes with dibutyryl- or 8-bromo cAMP also inhibited Pal-induced apoptosis (Fig. 2B). We further explored possible role of downstream cAMP effectors, namely, protein kinase A (PKA) and exchange protein activated by cAMP (EPAC) (Misra et al., 2005). We found that PKA inhibitor KT5720 partially blocked the protection by UDCA-LPE or dibutyryl cAMP (Fig. 2C). Western blot analyses of cleaved caspase 3 and PARP-1 proteins also revealed that KT5720 partially reversed the inhibition of these proteins by UDCA-LPE (Fig. 2D), indicating an involvement of PKA in lipoprotection by UDCA-LPE. We excluded an involvement of EPAC because an EPAC activator CPT-2-Me-cAMP did not inhibit Pal-induced apoptosis, and that an EPAC inhibitor BrefeldinA did not reverse the ability of UDCA-LPE to inhibit lipoapoptosis (Fig. 2E).

### **Effects of UDCA-LPE on triglycerides and fatty acid composition during lipoprotection.**

It is known that the treatment of cultured cells with MUFA, such as, oleate (18:1n-9) and palmitoleate (16:1n-7) used at 200  $\mu$ M is associated with accumulation TG (Listenberger et al., 2003; Li et al., 2009) and PL (Collins et al., 2010) concomitant with protection against lipotoxicity. We therefore determined whether UDCA-LPE could protect lipoapoptosis by modulating TG and PL levels. Treatment of mouse hepatocytes with Pal for 20 h elevated TG levels which were further elevated by UDCA-LPE co-treatment (Fig. 3A). Such further TG elevation was not observed upon treatment with 60  $\mu$ M UDCA, LPE, individually added UDCA + LPE, oleate or palmitoleate (Fig. 3B). Notably, treatment of hepatocytes with 75  $\mu$ M UDCA-LPE could cause a moderate increase of TG levels (Fig. 3A).

We next determined whether further elevation of TG was associated with alterations of fatty acid composition during lipoprotection by UDCA-LPE. By using GC-MS, Pal treatment of mouse hepatocytes for 20 h caused significant increases of saturated and 15-17-carbon fatty acids (Fig. 3C). UDCA-LPE co-treatment showed a trend for inhibition of these increases concomitant with a trend

for further increases of mono-, >2 unsaturated as well as 18-19- and 22-24-carbon fatty acids. Detailed analysis shown in Table 1 revealed that UDCA-LPE co-treatment reduced the levels of Pal (16:0) by ~27 nmol/mg protein (219.7±20 vs. 192.7±8.1 for Pal and Pal+UDCA-LPE, respectively). Concomitantly, the levels of oleate (18:1n-9) were further increased by ~21 nmol/mg protein (74.5±9.2 vs. 95.7±4.4 for Pal and Pal+UDCA-LPE, respectively). We investigated further whether UDCA-LPE molecule (which by itself contains oleate on the LPE moiety) could account for the observed increases of oleate. Intracellular concentrations of UDCA-LPE were found to be ~0.5 nmol/mg protein (Fig. 3D) being much lower than those of the increased oleate. With UDCA-LPE treatment alone, intracellular concentrations of UDCA (Fig. 3D) and total LPE (Table 2) were found to be similar to those of controls of ~0.3 and 1.55 nmol/mg protein, respectively, and the latter again could not account for the observed increased oleate. Thus, our data indicated an absence of UDCA-LPE hydrolysis to UDCA and LPE, which is consistent with our previous study using fluorescently labelled UDCA-LPE (Chamulitrat et al., 2009). These data were consistent with the observed optimal lipoprotection by intact UDCA-LPE, but not by its metabolite UDCA or LPE (Fig. 1F). Together with oleate (18:1n-9), UDCA-LPE co-treatment showed a trend to further increase the levels of homo- $\gamma$ -linoleate (20:3n-6), DPA (22:5n-3), and DHA (22:6n-3) (Table 1). The total fatty acid levels were increased upon Pal treatment, and these levels were not altered by UDCA-LPE co-treatment (Fig. 3E). Rather than by lowering the total fatty acid contents, UDCA-LPE protected lipoapoptosis by altering fatty acid composition. These alterations include the decreases of toxic SFA concomitant with marked increases of cytoprotective MUFA and to a lesser extent  $\omega$ -3 PUFA including DPA, and DHA.

### **Role of SCD-1 in UDCA-LPE lipoprotection.**

Mechanism for increases of TG during lipoprotection has been demonstrated to involve a conversion of SFA to MUFA by SCD-1 (Listenbeger et al., 2003; Collins et al., 2010). In the liver (Li et al.,

2009), MUFA provides metabolic adaptation for lipoprotection by incorporating SFA and MUFA into TG and PL. We therefore investigated possible role of SCD-1 during UDCA-LPE lipoprotection. We observed time-dependent regulation of SCD-1 on the mRNA and protein levels (Fig. 4A). Compared to Pal, UDCA-LPE co-treatment caused further increases of SCD-1 mRNA after 4 h and SCD-1 protein after 9 h. This may indicate early response for MUFA synthesis to elicit protection during apoptosis observable at 20 h. Treatment of mouse hepatocytes with Pal for 20 h markedly decreased SCD-1 mRNA expression, which was not rescued by UDCA-LPE co-treatment. This was likely due to an inhibition of SCD-1 transcription by PUFA (Ntambi, 1999), which had an increase trend following Pal treatment (Table 1). Co-treatment with LPE or individually added UDCA + LPE did not increase SCD-1 protein after 9 h treatment indicating the importance of intact UDCA-LPE in SCD-1 induction (Fig. 4B). Because cAMP/PKA pathway could in part play a role in UDCA-LPE lipoprotection (Fig. 2), a PKA inhibitor KT5720 was used to test whether there was a cross-talk between cAMP and SCD-1 pathways. We found that KT5720 treatment did not significantly block UDCA-LPE-dependent upregulation of SCD-1 protein detectable at 9 h or SCD-1 mRNA detectable at 4 h (Fig. 4B). This indicated that SCD-1 upregulation by UDCA-LPE co-treatment was unlikely to be mediated by cAMP and PKA.

We performed SCD-1 knockdown by using siRNAs to determine possible role of SCD-1 on UDCA-LPE lipoprotection (Fig. 4C). In our hands, siRNA only knocked down SCD1 protein by ~50% after 9 h treatment. Pal and UDCA-LPE co-treatment significantly increased SCD-1 protein expression in con siRNA-transfected cells, but failed to do so in SCD-1 siRNA-transfected cells. Compared to con siRNA-transfected cells, Pal treatment of SCD-1 knockdown cells caused markedly increased apoptosis, as seen by increased cleaved caspase 3 and cleaved PARP-1 protein expression (Fig. 4C), which was consistent with previous reports (Li et al., 2009). In SCD-1-knockdown cells, the ability of UDCA-LPE to inhibit apoptosis became weaker as quantitatively

demonstrated by caspase 3 activity assay (Fig. 4D, left). UDCA-LPE was found to inhibit apoptosis by ~60% in con siRNA-transfected cells, and to a lesser extent of ~40% in SCD-1 siRNA-1 or siRNA-2 transfected cells. Concomitantly, UDCA-LPE and Pal co-treatment significantly further increased TG levels in con siRNA-transfected cells (Fig. 4D, right), and the ability of UDCA-LPE to further increase TG became less effective with SCD-1 knockdown. Thus, SCD-1 may in part contribute to UDCA-LPE lipoprotection for increases of TG.

To explore possible mechanisms for increases of >2 unsaturated (Fig. 3C) as well as an increased trend of DPA (22:5n-3) and DHA (22:6n-3) (Table 1), we measured mRNA expression of fatty acid desaturase (Fads) and elongase (Elovl) (Green et al., 2010; Moon et al., 2009) genes. Similar to earlier observation of SCD-1 upregulation at 4 h, UDCA-LPE co-treatment further upregulated mRNA expression of Fads 1 (delta6 desaturation) (Fig. 5A) as well as Elovl 5 and 6 (Fig. 5B). Expression of Fads 2 (delta5 desaturation) was not affected by Pal or UDCA-LPE treatment. Expression of *de novo* lipogenesis genes fatty acid synthase (FAS) and acetyl-CoA carboxylase (ACC1) was further increased by UDCA-LPE co-treatment after 20 h treatment (Fig. 5C). Furthermore, expression of TG synthesis, lipolysis,  $\beta$ -oxidation, and metabolism transcription factor genes was measured in samples with 20 h treatment (Fig. 5D). Pal treatment decreased expression of diacylglycerol acyltransferase 1 (DGAT1) and liver X factor (LXR) which was rescued by UDCA-LPE co-treatment. UDCA-LPE co-treatment did not do so in expression of DGAT2, ATGL, Acox, PPAR $\alpha$ , PPAR $\gamma$ , and SREBP1c. Taken together, in addition of SCD-1 (delta9 desaturation) UDCA-LPE protection against Pal was thus associated with the rescues of Fads1, Elovl 5/6, DGAT1 and LXR by UDCA-LPE co-treatment, and this may account for increased PUFA contents (Fig. 3C and Table 1).

### **UDCA-LPE protects lipoapoptosis by modulating composition of phospholipids.**

It has been shown that Pal (16:0) is significantly incorporated into PL (Collins et al., 2010), we further characterized molecular species of PL in our samples by using ESI-MS/MS. Pal treatment increased total phosphatidylcholine (PC), and phosphatidylethanolamine (PE) levels (Table 2). UDCA-LPE co-treatment further increased the total PC (with a trend), and the total PS and LPE levels of ~5, 1.6, and 0.4 nmol/mg protein, respectively. Pal treatment increased the levels of SFA and MUFA in PC and PE (Table 2). UDCA-LPE co-treatment inhibited the increases of SFA while further increased MUFA levels in PC and PE supporting SCD-1 mechanism for protection. Pal treatment increased PUFA levels in PC and PS, while UDCA-LPE co-treatment further increased PUFA in PS, and with a trend in PC. Interestingly, LPE containing all SFA, MUFA, PUFA classes were increased during lipoprotection by UDCA-LPE, likely by SCD-1-independent mechanism, and this may additionally contribute to apoptosis inhibition which is shown to be mediated by MAPK (Nishina et al., 2006).

Further detailed analyses of PL molecular species shown in Table 3 revealed that UDCA-LPE lipoprotection was associated with decreased levels of PC and PE species containing 14:0, 16:0 and 18:0. This was concomitant with increased levels of PC, PE, PS, PI, and LPE containing SFA and MUFA or PUFA. MUFA was mainly 18:1n-9, and PUFA were mainly AA (20:4n-6), eicosapentaenoate (20:5n-3), DPA (22:5n-3), and DHA (22:6n-3). During protection, the predominant species most affected by UDCA-LPE were PC 34:1 (PC 16:0,18:1) and PC 34:2 (PC 16:0,18:2), indicating an efficient incorporation of 16:0 into PC. During lipoprotection by UDCA-LPE, the decreases of 16:0 and 18:0 fatty acids were also observed in ceramides and plasmalogen-based PE (Supplemental Table). During protection by UDCA-LPE, long-chain fatty acids, *i.e.*, 22:0, 20:4, 20:5, 22:5 and 22:6 were as well found to be increased in ceramides, sphingomyelin, plasmalogen-based PE and cholesterol.

### **Effects of UDCA-LPE on PL composition and comparison with UDCA, LPE and cAMP.**

Our GC-MS data in Table 1 revealed that UDCA-LPE treatment alone could increase the levels of oleate (18:1n-9) ( $68.8 \pm 5.9$  vs.  $89.2 \pm 12.1$  nmol/mg protein for con and UDCA-LPE, respectively). This prompted us to analyze the effects of UDCA-LPE alone on cellular fatty acid composition in details. Without Pal, UDCA-LPE treatment had a tendency to decrease Pal (16:0) levels (Table 1), but caused significant decreases of SFA in PC ( $1.87 \pm 0.1$  vs.  $1.04 \pm 0.13$  nmol/mg protein for con and UDCA-LPE, respectively) (Table 2). UDCA-LPE treatment alone caused an increase of PUFA observed only in PS ( $6.69 \pm 0.23$  vs.  $8.57 \pm 0.99$  nmol/mg protein for con and UDCA-LPE, respectively) (Table 2). This was the major contributor of the observed increased PUFA in PS when comparing between Pal and Pal+UDCA-LPE groups. The increases of PS by UDCA-LPE treatment alone corresponded to increases in PS 38:6, PS 40:6, and PS 42:6, most likely with combinations of 18:1,22:5 and 18:0,22:6 as the major species affected by UDCA-LPE (Table 3).

While UDCA-LPE treatment alone caused significant increases of oleate (18:1n-9) detectable by GC-MS (Table 1), these increases were not observed in any of the PL analyzed by ESI-MS/MS (Tables 2-3). The increases of oleate by UDCA-LPE treatment alone may correspond to previously observed increases of TG shown in Fig. 3A. Oleate generated by UDCA-LPE treatment may thus be readily incorporated into TG rather than PL pools.

Because LPE (Fig. 1F) and cAMP (Fig. 2B) was able to inhibit lipoapoptosis, we further compared alterations of fatty acid composition among UDCA-LPE, UDCA, LPE or cAMP by using GC-MS. Reported as % mol fatty acids, we found that treatment with UDCA-LPE or LPE for 20 h decreased cellular SFA, while increasing MUFA levels (Fig. 6A), and was consistent with the observed effects of UDCA-LPE shown in Table 1. Treatment with UDCA-LPE or LPE was able to increase oleate (18:1n-9) levels (Fig. 6B, left), suggesting a similar effect of LPE in stimulating MUFA synthesis which could account for partial protective effects of LPE (Fig. 1F). However,

UDCA-LPE was the only agent which increased the levels of >2 unsaturated fatty acids as seen by the increases of AA (20:4n-6) and DHA (22:6n-3) (Fig. 6B, right). These increases corresponded well with the observed upregulation of Fads1, Elovl6 and Elovl5 mRNA by UDCA-LPE treatment alone (Fig. 5 A and B). Treatment with UDCA did not cause any alterations of fatty acid composition, while that of 8-bromo cAMP decreased oleate, AA and DHA levels. The action of cAMP as a mediator of lipoprotection (Fig. 2) was unlikely related to the observed alteration of lipid metabolism (Fig. 3C and Tables 1-3) and SCD-1 (Fig. 4). Taken together, UDCA-LPE may exhibit maximal protection against Pal-induced apoptosis by two independent mechanisms, namely, cAMP/PKA signalling and alterations of fatty acid composition as outlined in Fig. 6C.

## Discussion

It is accepted that, not only the quantity of dietary fat, but also the type of fat contributes to the onset and progression from steatosis to NASH. The liver plays a central role in whole body lipid metabolism and responds rapidly to changes in dietary fat composition. Strategies for development of therapeutic agents should involve the lowering of hepatic toxic SFA and at the same time inhibiting key deleterious events occurring in NASH. We here demonstrated that UDCA-LPE inhibited Pal-induced apoptosis in mouse hepatocytes while altering the composition of fatty acids such that total contents of TG and PL were accumulated. Lipidomic data revealed that this protection was accompanied with increases of mainly oleate (18:1n-9), DPA (22:5n-3) and 22:6n-3 (DHA). Our study delineated molecular therapeutic pathways in UDCA-LPE's ability to inhibit lipoapoptosis by modulating composition of fatty acids in part via SCD-1 pathway, and as a minor mechanism by inducing cAMP/PKA signalling (Fig. 6C).

UDCA-LPE was active as an intact compound in inhibiting Pal-induced apoptosis which is in line with our previous studies (Chamulitrat et al., 2009). This exemplifies the significance of UDCA and LPE conjugation rendering its superiority over unconjugated bile acid (Pellicciari et al., 2004),



and a preference of PL for conjugation (Miller et al., 2007). Conjugated bile acids have been shown to activate receptor tyrosine kinases and intracellular signaling pathways in a G-protein coupled receptor (GPCR)-dependent manner (Hutchinson et al., 2008). GPCR activation leads to an elevation of cAMP (Hutchinson et al., 2008) which mediates apoptosis inhibition (Kwon et al., 2004; Webster et al., 1998). The observed UDCA-LPE lipoprotection via cAMP/PKA signalling supports a possibility that UDCA-LPE may interact with specific GPCRs. Among them are lipid-sensing GPCRs, *e.g.*, sphingosine-1-phosphate receptor 2 (Studer et al., 2012), and adenosine A2a receptor (Imarisio et al., 2012). UDCA-LPE (or cAMP generated by UDCA-LPE) may interact with these GPCRs to induce PKA signalling leading to activation of cytoprotective signals Akt and ERK (Dent et al., 2005). UDCA-LPE indeed induces Akt and ERK activation (Chamulitrat et al., 2009).

During lipoprotection (Fig. 6C), GC-MS and ESI-MS/MS analyses showed that UDCA-LPE increased elongation from Pal (16:0) to stearate (18:0), which was converted to oleate (18:1n-9) by SCD-1 (Listenberger et al., 2003; Collins et al., 2010). As we observed increases of Fads1 and Elovl 5/6 during lipoprotection by UDCA-LPE, elongation and desaturation of linoleate (18:2n-6) and linolenate (18:3n-3) generates AA (20:4n-6), 22:5n-3 and 22:6n-3 as end products of PUFA syntheses (Green et al., 2010; Moon et al., 2009). Furthermore, the increases of these  $\omega$ -3 PUFA were uniquely specific for UDCA-LPE particularly in PS pool. UDCA-LPE lipoprotection was associated with reduction of toxic SFA concomitant with increases of MUFA in PC and PE as well as increases of PUFA in PC and PS. We also observed further elevation of TG levels during UDCA-LPE lipoprotection. We did not perform detailed fatty acid analysis of TG pools, however, TG containing very long-chain fatty acids have previously been shown to be associated with protection (Hall et al., 2010). The further elevation of TG by UDCA-LPE co-treatment was found to be on the order of  $\sim 1$   $\mu\text{mol/mg}$  protein (Fig. 3A-B). This correlates with the rescues of reduced expression of DGAT1 and metabolic nuclear receptor LXR (Fig. 5D). Further studies are needed to determine

whether UDCA-LPE is an LXR agonist which may mediate protective actions of  $\omega$ -3 PUFA (Jung et al., 2011). Incorporation of fatty acids into TG can play as a major contribution in diverting SFA away from apoptosis pathways. This is supported by previous data showing that inhibition of TG accumulation in obese mice worsens liver damage (Yamaguchi et al., 2007). Among PL types, PC and LPE were mostly affected during lipoprotection by UDCA-LPE. The metabolically generated LPE may additionally contribute to lipoprotection of UDCA-LPE (Nishina et al., 2006). The observed increases of the predominant PC 34:1 (most likely 16:0,18:1) species showed that Pal and oleate were readily incorporated into PC, and again diverting Pal away from apoptosis. Our current data are consistent with the notion that PC species are indeed protective against steatosis (Niebergall et al., 2011). PC containing MUFA are present in higher concentrations in cells overexpressed with anti-apoptosis Bcl-2 (Cantrel et al., 2009). Furthermore, heat stress has been shown to increase contents of saturated fatty acids while decrease those of PUFA particularly AA (20:4n-6) (Balogh et al., 2010). Associated with protection, increases of PUFA, such as, AA, DPA and DHA were observed not only in PL but also PE-based plasmalogen pools (Wallner et al., 2011). These PUFA-containing lipids may alter membrane lipid remodelling and protect cells by increasing membrane fluidity (Stubbs and Smith, 1984).

Interestingly, AA (20:4n-6), DPA (22:5n-3) and DHA (22:6n-3) were identified as the main PUFA which were increased by UDCA-LPE treatment alone in a similar way as those fatty acids found during UDCA-LPE lipoprotection (Table 3). These increases of PUFA may be due to the ability of UDCA-LPE to upregulate Fads1, Elovl 6, FAS, and PPAR $\gamma$  mRNA expression (Fig. 5). These increases were uniquely specific for UDCA-LPE as its metabolite UDCA, LPE or cAMP with lesser effectiveness in apoptosis inhibition did not increase these PUFA. UDCA-LPE alone increased DPA (22:5n-3) and DHA (22:6n-3) contents in PS, thus supporting the importance of these species to play a role in cytoprotection (Kim et al., 2010). DHA is a precursor of potent anti-inflammatory

signalling molecules (Moon et al., 2009; Kim et al., 2010). As  $\omega$ -6 and  $\omega$ -3 PUFA are key components of membrane PL, their levels are known to be decreased in livers of NASH patients (Puri et al., 2007). Administration of DHA (22:6n-3) in NASH mice (Depner et al., 2013) and in children with fatty liver (Nobili et al., 2011) has been shown to be beneficial for treatment of this liver disease. UDCA-LPE's ability to increase DHA bolsters its therapeutic use by strengthening PL membranes, increasing cell membrane fluidity, and replenishing the depleted DHA in NASH livers. Under *in vivo* conditions, TG and PL may be hydrolyzed by lipases and phospholipases to release free  $\omega$ -3 PUFA which can be subjected to  $\beta$ -oxidation (Hall et al., 2010). AA (20:4n-6) and DHA (22:6n-3) have been shown to suppress nuclear SREBP-1c (Ntambi, 1999; Moon et al., 2009; Jump et al., 2008), which in turn leads to decreased transcription of *de novo* lipogenesis genes *in vivo*. Consistently, we found that *de novo* lipogenesis gene expression in livers of mice fed with high-fat diet was markedly inhibited upon chronic treatment with UDCA-LPE (Pathil et al., 2012).

In conclusion, UDCA-LPE protected lipoapoptosis by inducing a shift in fatty acid content towards MUFA and PUFA for incorporation into TG and PL concomitant with decreased Pal and SFA and rendering them unavailable for apoptosis. UDCA-LPE protected apoptosis by uniquely increasing PUFA in PC and PS for cell membrane remodelling and stabilization. Our *in vitro* results provide mechanistic insights of a drug candidate UDCA-LPE for treatment of NASH by its unique metabolic reprogramming that minimize damage brought on by excessive SFA.

## **Acknowledgments**

We thank Nenad Katava for technical assistance and Dr. W. Hartmann for statistical analyses.

## **Authorship contributions**

*Participated in research design:* Chamulitrat, Xu, Pathil, Stremmel.

*Conducted experiments:* Xu, Gan-Schreier, Liebisch, Pathil.

*Contributed new reagents or analytic tools:* Liebisch, Schmitz, Pathil, Gan-Schreier, Stremmel.

*Performed data analysis:* Chamulitrat, Xu, Liebisch, Gan-Schreier.

*Wrote or contributed to the writing of the manuscript:* Chamulitrat, Liebisch, Xu, Stremmel

## References

- Balakrishnan A, Wring SA, Coop A, and Polli JE (2006) Influence of charge and steric bulk in the C-24 region on the interaction of bile acids with human apical sodium-dependent bile acid transporter. *Mol Pharm.* **3**: 282-292.
- Balogh G, Péter M, Liebisch G, Horváth I, Török Z, Nagy E, Maslyanko A, Benko S, Schmitz G, Harwood JL, and Víg L. (2010) Lipidomics reveals membrane lipid remodelling and release of potential lipid mediators during early stress responses in a murine melanoma cell line. *Biochim Biophys Acta.* **1801**: 1036-1047.
- Beraza N, Ofner-Ziegenfuss L, Ehedeo H, Boekschoten M, Bischoff SC, Mueller M, Trauner M, and Trautwein C. (2011) Nor-ursodeoxycholic acid reverses hepatocyte-specific nemo-dependent steatohepatitis. *Gut.* **60**: 387-396.
- Briz O, Serrano MA, Rebollo N, Hagenbuch B, Meier PJ, and Koepsell H (2002) Carriers involved in targeting the cytostatic bile acid-cisplatin derivatives cis-diammine-chloro-cholyglycinate-platinum(II) and cis-diammine-bisursodeoxycholate-platinum(II) toward liver cells. *Mol Pharmacol.* **61**: 853-860.
- Cantrel C, Zachowski A, and Geny B (2009) Over-expression of the anti-apoptotic protein Bcl-2 affects membrane lipid composition in HL-60 cells. *Lipids.* **44**: 499-509.
- Chamulitrat W, Burhenne J, Rehlen T, Pathil A, and Stremmel W (2009) Bile salt-phospholipid conjugate ursodeoxycholyly lysophosphatidylethanolamide as a hepatoprotective agent. *Hepatology.* **50**: 143-154.
- Chamulitrat W, Zhang W, Xu W, Pathil A., Setchell K, and Stremmel W (2012) Hepatoprotectant ursodeoxycholyly lysophosphatidylethanolamide increasing phosphatidylcholine levels as a potential therapy of acute liver injury. *Front Physiol.* **3**: 24-32.

- Collins JM, Neville MJ, Hoppa MB, Frayn KN (2010) De novo lipogenesis and stearoyl-CoA desaturase are coordinately regulated in the human adipocyte and protect against palmitate-induced cell injury. *J Biol Chem.* **285**: 6044-6052.
- Dent P, Fang Y, Gupta S, Studer E, Mitchell C, Spiegel S, and Hylemon PB. (2005) Conjugated bile acids promote ERK1/2 and AKT activation via a pertussis toxin-sensitive mechanism in murine and human hepatocytes. *Hepatology.* **42**: 1291-1299.
- Depner CM, Philbrick KA, and Jump DB (2013) Docosahexaenoic Acid Attenuates Hepatic Inflammation, Oxidative Stress, and Fibrosis without Decreasing Hepatosteatosis in Ldlr-/- Mouse Model of Western Diet-Induced Nonalcoholic Steatohepatitis. *J Nutr.* **143**: 315-323.
- Diehl AM (1999) Non-alcoholic fatty liver disease. *Semin Liver Dis.* **19**: 221-219.
- Ecker J, Scherer M, Schmitz G, and Liebisch G (2012) A rapid GC-MS method for quantification of positional and geometric isomers of fatty acid methyl esters. *J Chromatogr B Analyt Technol Biomed Life Sci.* **897**: 98-104.
- Fickert P, Wagner M, Marschall HU, Fuchsbichler A, Zollner G, Tsybrovskyy O, Zatloukal K, Liu J, Waalkes MP, Cover C, Denk H, Hofmann AF, Jaeschke H, and Trauner M. (2006) 24-norUrsodeoxycholic acid is superior to ursodeoxycholic acid in the treatment of sclerosing cholangitis in Mdr2 (Abcb4) knockout mice. *Gastroenterology.* **130**: 465-481.
- Goto M, Okamoto Y, Yamamoto M, and Aki H (2001) Anti-inflammatory effects of 5-aminosalicylic acid conjugates with chenodeoxycholic acid and ursodeoxycholic acid on carrageenan-induced colitis in guinea-pigs. *J Pharm Pharmacol.* **53**: 1711-1720.
- Green CD, Ozguden-Akkoc CG, Wang Y, Jump DB, and Olson LK (2010) Role of fatty acid elongases in determination of de novo synthesized monounsaturated fatty acid species. *J Lipid Res.* **51**: 1871-1877.

- Hall D, Poussin C, Velagapudi VR, Empsen C, Joffraud M, Beckmann JS, Geerts AE, Ravussin Y, Ibberson M, Oresic M, and Thorens B. (2010) Peroxisomal and microsomal lipid pathways associated with resistance to hepatic steatosis and reduced pro-inflammatory state. *J Biol Chem.* **285**: 31011-31023
- Hutchinson DS, Summers RJ, and Bengtsson T (2008) Regulation of AMP-activated protein kinase activity by G-protein coupled receptors: potential utility in treatment of diabetes and heart disease. *Pharmacol Ther.* **119**: 291-310.
- Imarisio C, Alchera E, Sutti S, Valente G, Boccafoschi F, Albano E, and Carini R. (2012) Adenosine A2a receptor stimulation prevents hepatocyte lipotoxicity and non-alcoholic steatohepatitis (NASH) in rats. *Clin Sci (Lond).* **123**: 323-332.
- Jump DB, Botolin D, Wang Y, Xu J, Demeure O, and Christian B (2008) Docosahexaenoic acid (DHA) and hepatic gene transcription. *Chem Phys Lipids.* **153**: 3-13.
- Jung UJ, Millman PN, Tall AR, and Deckelbaum RJ. (2011) n-3 fatty acids ameliorate hepatic steatosis and dysfunction after LXR agonist ingestion in mice. *Biochim Biophys Acta.* **181**: 491-497.
- Kim HY, Akbar M, and Kim YS (2010) Phosphatidylserine-dependent neuroprotective signaling promoted by docosahexaenoic acid. *Prostaglandins Leukot Essent Fatty Acids.* **82**: 165-172.
- Kwon G, Pappan KL, Marshall CA, Schaffer JE, and McDaniel ML (2004) cAMP Dose-dependently prevents palmitate-induced apoptosis by both protein kinase A- and cAMP-guanine nucleotide exchange factor-dependent pathways in beta-cells. *J Biol Chem.* **279**: 8938-8945.
- Li Z, Agellon LB, Allen TM, Umeda M, Jewell L, Mason A, and Vance DE (2006) The ratio of phosphatidylcholine to phosphatidylethanolamine influences membrane integrity and steatohepatitis. *Cell Metab.* **3**: 321-331.

- Li, ZZ, Berk M, McIntyre TM, and Feldstein AE (2009) Hepatic lipid partitioning and liver damage in nonalcoholic fatty liver disease: role of stearoyl-CoA desaturase. *J Biol Chem.* **284**: 5637-5644.
- Liebisch G, Lieser B, Rathenber J, Drobnik W, and Schmitz G (2004) High-throughput quantification of phosphatidylcholine and sphingomyelin by electrospray ionization tandem mass spectrometry coupled with isotope correction algorithm. *Biochim Biophys Acta.* **1686**: 108-117.
- Listenberger LL, Han X, Lewis SE, Cases S, Farese RV.Jr, Ory DS, Schaffer JE (2003) Triglyceride accumulation protects against fatty acid-induced lipotoxicity. *Proc Natl Acad Sci U S A.* **100**: 3077-3082.
- Maeda K., Kambara M, Tian Y, Hofmann AF, and Sugiyama Y (2006) Uptake of ursodeoxycholate and its conjugates by human hepatocytes: role of Na(+)-taurocholate cotransporting polypeptide (NTCP), organic anion transporting polypeptide (OATP) 1B1 (OATP-C), and oatp1B3 (OATP8). *Mol Pharm.* **3**: 70-77.
- Miller SD, Greene CM, McLean CM, Lawless W, Taggart CC, O'Neill SJ, and McElvaney NG (2007) Tauroursodeoxycholic acid inhibits apoptosis induced by Z alpha-1 antitrypsin via inhibition of Bad. *Hepatology.* **46**: 496-503.
- Misra UK, and Pizzo SV (2005) Coordinate regulation of forskolin-induced cellular proliferation in macrophages by protein kinase A/cAMP-response element-binding protein (CREB) and Epac1-Rap1 signaling: effects of silencing CREB gene expression on Akt activation. *J Biol Chem.* **280**: 38276-38289.
- Moon YA, Hammer RE, and Horton JD (2009) Deletion of ELOVL5 leads to fatty liver through activation of SREBP-1c in mice. *J Lipid Res.* **50**: 412-423.



- Niebergall LJ, Jacobs RL, Chaba T, and Vance DE. (2011) Phosphatidylcholine protects against steatosis in mice but not non-alcoholic steatohepatitis. *Biochim Biophys Acta*. **1811**: 1177-1185.
- Nishina A, Kimura H, Sekiguchi A, Fukumoto RH, Nakajima S, Furukawa S (2006) Lysophosphatidylethanolamine in *Grifola frondosa* as a neurotrophic activator via activation of MAPK. *J Lipid Res*. **47**: 1434-1443.
- Nobili V, Bedogni G, Alisi A, Pietrobattista A, Risé P, Galli C. and Agostoni C (2011) Docosahexaenoic acid supplementation decreases liver fat content in children with non-alcoholic fatty liver disease: double-blind randomised controlled clinical trial. *Arch Dis Child*. **96**: 350-353.
- Ntambi JM (1999) Regulation of stearyl-CoA desaturase by polyunsaturated fatty acids and cholesterol. *J Lipid Res*. **40**: 1549-1558.
- Pathil A, Mueller J, Warth A, Chamulitrat W, and Stremmel W (2012) Ursodeoxycholyl lysophosphatidylethanolamide improves steatosis and inflammation in murine models of nonalcoholic fatty liver disease. *Hepatology*. **55**: 1369-1378.
- Pathil A, Warth A, Chamulitrat W, and Stremmel W (2011) The synthetic bile acid-phospholipid conjugate ursodeoxycholyl lysophosphatidylethanolamide suppresses TNF $\alpha$ -induced liver injury. *J Hepatol*. **54**: 674-684.
- Pellicciari R, Costantino G, Camaioni E, Sadeghpour BM, Entrena A, Willson TM, and Fiorucci S (2004) Bile acid derivatives as ligands of the farnesoid X receptor. Synthesis, evaluation, and structure-activity relationship of a series of body and side chain modified analogues of chenodeoxycholic acid. *J Med Chem*. **47**: 4559-4569.
- Puri P, Baillie RA, Wiest MM, Mirshahi F, Choudhury J, Cheung O, Sargeant C, Contos MJ, and Sanyal AJ (2007) A lipidomic analysis of nonalcoholic fatty liver disease. *Hepatology*. **46**: 1081-1090.

- Rahman SM, Qadri I, Janssen RC, and Friedman JE (2009) Fenofibrate and PBA prevent fatty acid-induced loss of adiponectin receptor and pAMPK in human hepatoma cells and in hepatitis C virus-induced steatosis. *J Lipid Res.* **50**: 2193-2202.
- Ratziu V, Caldwell S, and Neuschwander-Tetri BA (2010) Therapeutic trials in nonalcoholic steatohepatitis: insulin sensitizers and related methodological issues. *Hepatology.* **52**: 2206-2215.
- Ratziu V, de Ledinghen V, Oberti F, Mathurin P, Wartelle-Bladou C, Renou C, Sogni P, Maynard M, Larrey D, Serfaty L, Bonnefont-Rousselot D, Bastard JP, Rivière M, and Spénard J; FRESGUN. (2011) A randomized controlled trial of high-dose ursodeoxycholic acid for nonalcoholic steatohepatitis. *J Hepatol.* **54**: 1011-1019.
- Rodrigues CM, Fan G, Wong PY, Kren BT, and Steer CJ (1998) Ursodeoxycholic acid may inhibit deoxycholic acid-induced apoptosis by modulating mitochondrial transmembrane potential and reactive oxygen species production. *Mol Med.* **4**: 165-178.
- Satapathy SK, and Sanyal AJ (2010) Novel treatment modalities for nonalcoholic steatohepatitis. *Trends Endocrinol Metab.* **21**: 668-675.
- Stubbs CD, and Smith AD (1984) The modification of mammalian membrane polyunsaturated fatty acid composition in relation to membrane fluidity and function. *Biochim Biophys Acta.* **779**: 89-137.
- Studer E, Zhou X, Zhao R, Wang Y, Takabe K, Nagahashi M, Pandak WM, Dent P, Spiegel S, Shi R, Xu W, Liu X, Bohdan P, Zhang L, Zhou H, and Hylemon PB (2012) Conjugated bile acids activate the sphingosine-1-phosphate receptor 2 in primary rodent hepatocytes. *Hepatology.* **55**: 267-276.
- Tsochatzis EA, Gurusamy KS, Gluud C, and Burroughs AK (2009) Ursodeoxycholic acid and primary biliary cirrhosis: EASL and AASLD guidelines. *J Hepatol.* **51**: 1084-1085.

Wallner S, and Schmitz G (2011) Plasmalogens the neglected regulatory and scavenging lipid species. *Chem Phys Lipids*. **164**: 573-589.

Webster CR, and Anwer MS (1998) Cyclic adenosine monophosphate-mediated protection against bile acid-induced apoptosis in cultured rat hepatocytes. *Hepatology*. **27**: 1324-1331.

Yamaguchi K, Yang L, McCall S, Huang J, Yu XX, Pandey, S.K. Bhanot S, Monia BP, Li YX, and Diehl AM.. (2007) Inhibiting triglyceride synthesis improves hepatic steatosis but exacerbates liver damage and fibrosis in obese mice with nonalcoholic steatohepatitis. *Hepatology*. **45**: 1366-1374

Zhang LX, Liang TJ, Tan YR, Ren WH, Han GQ, Zhang J, Wang LC, and Qin CY (2010) Protective effects of ursodeoxycholic acid against immune-mediated liver fibrosis in rats. *Hepatology*. **57**: 1196-1202.

### **Footnotes**

This study was supported by Deutsche Forschungsgemeinschaft [STR 216/15-3]; European Community's Seventh Framework Programme IP-Project Lipidomic Net [FP7/2007-2013-202272]. Part of this work was presented as a poster at European Association for the Study of the Liver 2011, Berlin. Reprint requests should be sent to Dr. Walee Chamulitrat, Im Neuenheimer Feld 345 EG, 69120 Heidelberg, Germany. Tel: 049-6221-56-38731; Fax: 049-6221-56-5398; email: Walee.Chamulitrat@med.uni-heidelberg.de.

### Figure Legends

**Fig. 1.** (A) Chemical structure of UDCA-LPE. (B) Treatment of mouse hepatocytes with 300  $\mu$ M palmitic acid (Pal) for 20 h increased expression of pro-apoptotic proteins Bim, cleaved caspase 3 (17 and 19 kDa), and cleaved PARP-1 (25 kDa). Co-treatment with 60  $\mu$ M UDCA-LPE markedly inhibited their expression. Data were representatives from 3 hepatocyte preparations. (C) UDCA-LPE at 50 or 75  $\mu$ M co-treated with Pal inhibited caspase 3 activity. (D) Dose response of UDCA-LPE lipoprotection with  $IC_{50}$   $\sim$ 32  $\mu$ M. (E) Co- and 1 h-pre-treatment of UDCA-LPE with Pal were required for optimal protection. (F) UDCA-LPE as an intact molecule was required for apoptosis inhibition. (G) For inhibition of caspase 3 activity, UDCA-LPE was more potent than chenodeoxycholate (CDCA) or taurine-conjugated UDCA (tauro-UDCA) when used at 60  $\mu$ M. Data were mean  $\pm$  SD, N=6; \*\*\*,  $p$ <0.001 versus con; †,  $p$ <0.05 versus Pal.

**Fig. 2.** Lipoprotection by UDCA-LPE in mouse hepatocytes in part involves c-AMP/PKA signalling. (A) After 30 min treatment, 25, 75 or 100  $\mu$ M UDCA-LPE stimulated intracellular cAMP levels, while 100  $\mu$ M UDCA had a weak effect. (B) Co-treatment with 100  $\mu$ M dibutyryl or 800  $\mu$ M 8-bromo cAMP for 20 h markedly inhibited Pal-induced caspase 3 activities in a similar manner as 60  $\mu$ M UDCA-LPE. (C) Inhibition of lipoapoptosis by 60  $\mu$ M UDCA-LPE or 100  $\mu$ M dibutyryl cAMP was partially blocked by PKA inhibitor KT5720. KT5720 at 5  $\mu$ M was pre-treated 30 min prior to Pal addition. (D) UDCA-LPE inhibited Pal-induced upregulation of cleaved caspase 3 and cleaved PARP-1 proteins after 15 h. This inhibition was partially blocked by 30-min pretreatment with 10  $\mu$ M KT5720. (E) An EPAC activator 8-(4-chlorophenylthio)-2'-O-methyladenosine 3',5'-cyclic monophosphate (CPT-2-Me-cAMP) used at 20  $\mu$ M did not inhibit Pal-induced apoptosis after 20 h. An EPAC inhibitor brefeldin A used at 100  $\mu$ M with 1 h pretreatment did not

reverse protective effects by UDCA-LPE. Data were mean  $\pm$  SD, N=6; \*,  $p<0.05$ , \*\*\*,  $p<0.001$  versus con; †,  $p<0.05$  versus Pal; §,  $p<0.05$  versus Pal + UDCA-LPE or Pal + dibutyl cAMP.

**Fig. 3.** Lipoprotection by UDCA-LPE is concomitant with increased triglycerides and alterations of fatty acid composition. (A) Pal treatment of mouse hepatocytes induced increase of TG levels which were further increased by co-treatment with 50 or 75  $\mu$ M UDCA-LPE. (B) The increases of TG levels were found only when Pal was co-treated with 60  $\mu$ M UDCA-LPE, but not with 60  $\mu$ M LPE, UDCA, individually added UDCA+LPE, oleate or palmitoleate. (C) By GC-MS analyses, Pal treatment increased (left panel) saturated (sat), mono-unsaturated and >2 unsaturated fatty acids as well as (right panel) 15-17 and 22-24 carbon fatty acids. UDCA-LPE co-treatment showed a trend for inhibition of sat and 15-17 carbon fatty acids concomitant with further increases of mono-unsaturated, >2 unsaturated fatty acids, 18-19, and 22-24 carbon fatty acids. (D) Intracellular concentrations of UDCA-LPE and UDCA with 60  $\mu$ M UDCA-LPE treatment for 12 or 20 h were ~0.3-0.5 nmol/mg protein. (E) The increased total fatty acid concentrations by Pal were not altered by UDCA-LPE co-treatment. Data were mean  $\pm$  SD, N=4-6; \*,  $p<0.05$ ; \*\*\*,  $p<0.001$  versus con; †,  $p<0.05$  versus Pal.

**Fig. 4.** Role of SCD-1 during lipoprotection by UDCA-LPE in mouse hepatocytes. (A) UDCA-LPE and Pal co-treatment increased SCD-1 mRNA expression after 4 h (left panel) and SCD-1 protein after 9 h (right panel). (B) After 9 h treatment, LPE or individually added UDCA + LPE did not upregulate SCD-1 protein (left panel). UDCA-LPE's ability to up-regulate SCD-1 protein (middle) and mRNA (right) after 9 and 4 h co-treatment respectively, was not significantly modified by 30 min-pretreatment with 5 or 10  $\mu$ M KT5720. (C) After 9 h treatment, SCD-1 siRNA-transfected cells showed decreased SCD-1 protein compared to

con siRNA-transfected cells. This was concomitant with increased cleaved caspase 3 and cleaved PARP-1 protein expression in the corresponding treatment group. (D) The ability of UDCA-LPE to inhibit lipoapoptosis (2 left panels) and to increase triglycerides (2 right panels) was decreased upon SCD-1 knockdown using SCD1 siRNA-1 and SCD1 siRNA-2. Data are mean  $\pm$  SD, N=4; \*,  $p < 0.05$  versus con; †,  $p < 0.05$  versus Pal, or con siRNA.

**Fig. 5.** Alterations of lipid metabolism genes during lipoprotection by UDCA-LPE. Mouse hepatocytes were treated with 300  $\mu$ M palmitate (Pal) with co-treatment with 60  $\mu$ M UDCA-LPE for 4 or 20 h. (A) Fatty acid desaturase (Fads) 1 but not Fads 2 mRNA expression was increased after 4 h treatment. (B) Expression of elongase 6 (Elovl6) mRNA was elevated by UDCA-LPE and Pal co-treatment after 4 and 20 h. (C) Pal treatment for 20 h increased FAS and ACC1 expression which was further increased by UDCA-LPE co-treatment. (D) Pal treatment for 20 h lowered expression of DGAT 1 and LXR which was rescued by UDCA-LPE co-treatment. UDCA-LPE co-treatment with Pal did not modify DGAT2, ATGL, Acox, PPAR $\gamma$ , PPAR $\alpha$ , and SREBP1c after 20 h treatment. Data were mean  $\pm$  SD, N=3-4, except data in D (quadruplet PCRs) were representatives from 2 experiments; \*,  $p < 0.05$ ; \*\*,  $p < 0.01$  versus con; †,  $p < 0.05$  versus Pal.

**Fig. 6.** Effects of UDCA-LPE, its metabolites, and cAMP on fatty acid composition of mouse hepatocytes. (A) Based on % mol fatty acids, treatment of mouse hepatocytes with 60  $\mu$ M UDCA-LPE or LPE for 20 h caused marked decreases of saturated fatty acids concomitant with increases of mono-unsaturated fatty acids. The opposite was found for 800  $\mu$ M 8-bromo cAMP treatment. (B) UDCA-LPE or LPE treatment for 20 h increased oleate levels. UDCA-LPE was the only compound which increased levels of AA and DHA, while 8-bromo cAMP decreased these levels. (C) Proposed mechanisms for UDCA-LPE protection against Pal-induced apoptosis in mouse hepatocytes include a minor pathway involving cAMP/PKA

signalling, and alterations of fatty acid composition as a major pathway. UDCA-LPE co-treatment with Pal caused a shift of fatty acid metabolism from SFA to MUFA and PUFA. These were concomitant with increased TG and PL. The latter were observed in various PC, PE, PS, PI, and LPE species. Data were mean  $\pm$  SD in A and B, N=3; \*,  $p < 0.05$  versus con.



Table 1 Total fatty acid composition during lipoapoptosis and protection by UDCA-LPE<sup>a</sup>.

Fatty acids	con	Pal	Pal		Changes in
			+UDCA-LPE	UDCA-LPE	nmol/mg protien
Lauric acid (12:0)	4.1 ± 0.6	3.5 ± 0.1	4.0 ± 0.3	2.6 ± 1.0*	ns
Myristic acid (14:0)	3.8 ± 2.7	5.1 ± 0.6	0.0 ± 0.0 <sup>†</sup>	3.9 ± 2.3	↓ 5.0
Palmitic acid (16:0)	113.6 ± 6.8	219.7 ± 20*	192.7 ± 8.1* <sup>†</sup>	95.2 ± 57.3	↓ 27
Sapienic acid (16:1n-10)	0.6 ± 0.1	1.0 ± 0.2*	0.9 ± 0.00*	0.6 ± 0.2	↓ 0.2
Palmitoleic acid (16:1n-7)	10.2 ± 0.9	24.1 ± 3.2*	20.3 ± 1.1*	7.7 ± 6.8	↓ 3.9
Stearic acid (18:0)	61.2 ± 2.5	62.0 ± 2.1	64.1 ± 3.6	51.5 ± 11.5*	ns
Oleic acid (18:1n-9)	68.8 ± 5.9	74.5 ± 9.2	95.7 ± 4.4* <sup>†</sup>	89.2 ± 12.1*	↑ 21.2
Vaccenic acid (18:1n-7)	6.3 ± 0.4	7.1 ± 0.6	6.7 ± 0.3	5.0 ± 1.2	ns
Linoleic acid (18:2n-6)	54.4 ± 3.7	59.5 ± 3.9	63.1 ± 2.4	44.4 ± 13.7	ns
Linolenic acid (18:3n-3)	3.1 ± 0.3	3.3 ± 0.4	3.7 ± 0.2	2.3 ± 0.9	ns
Arachidic acid (20:0)	3.63 ± 0.4	1.3 ± 0.07*	1.4 ± 0.0*	2.9 ± 1.0*	ns
Gondoic acid (20:1n-9)	1.6 ± 0.2	1.2 ± 0.1*	1.3 ± 0.1	2.2 ± 0.6*	ns
homo-γ-linoleic acid (20:3n-6)	4.9 ± 0.3	5.1 ± 0.2	5.6 ± 0.3	4.8 ± 1.0	ns
Arachidonic acid (20:4n-6)	33.3 ± 1.8	37.7 ± 1.6	41.4 ± 2.8*	33.0 ± 8.1	ns
Docosapentaenoic acid (22:5n-3)	2.4 ± 0.3	2.7 ± 0.2	3.1 ± 0.2*	2.1 ± 0.7	ns
Docosahexaenoic acid (22:6n-3)	20.3 ± 2.0	22.4 ± 1.3	25.8 ± 1.6*	21.9 ± 4.7	ns

<sup>a</sup> Fatty acids were measured by GC-MS. Mouse hepatocytes were treated with 300 μM palmitate (Pal) with or without 60 μM UDCA-LPE for 20 h. All groups contained 0.5% BSA and 0.1% ethanol. Data were mean ± SD, N=4. All values were reported in nmol/mg protein. Significant difference: \*, *p*<0.05, con versus Pal, Pal+UDCA-LPE or UDCA-LPE; †, *p*<0.05, Pal versus Pal+UDCA-LPE. ns means not significant.

Table 2 Fatty acid saturation of phospholipids during lipopoptosis and protection by UDCA-LPE<sup>a</sup>.

PL class <sup>b</sup>	Fatty acid saturation <sup>b</sup>	con	Pal	Pal +UDCA-LPE	UDCA-LPE	Changes Pal+UDCALPE vs. Pal in nmol/mg protein
PC	SFA	1.87 ± 0.10	6.81 ± 0.24*	5.35 ± 0.12*†	1.04 ± 0.13*	↓
	MUFA	11.37 ± 0.32	15.34 ± 0.40*	18.22 ± 0.59*†	9.61 ± 1.31*	↑
	PUFA	42.71 ± 1.05	46.54 ± 1.92*	50.32 ± 2.15*	39.97 ± 5.61	ns
	total PC	57.53 ± 1.22	70.47 ± 2.48*	75.74 ± 2.91*	51.61 ± 7.00	ns
PE	SFA	0.15 ± 0.01	1.80 ± 0.05*	1.11 ± 0.03*†	0.10 ± 0.01	↓
	MUFA	0.43 ± 0.01	1.50 ± 0.02*	1.56 ± 0.02*	0.40 ± 0.06	↑
	PUFA	29.03 ± 0.67	32.39 ± 1.63	34.90 ± 1.53*	32.67 ± 4.67	ns
	total PE	32.84 ± 0.75	38.61 ± 1.80*	40.92 ± 1.68*	37.83 ± 5.39	ns
PS	MUFA	0.19 ± 0.08	0.09 ± 0.01*	0.08 ± 0.01*	0.06 ± 0.01*	ns
	PUFA	6.69 ± 0.23	7.40 ± 0.19*	9.00 ± 0.33*†	8.57 ± 0.99*	↑
	total PS	6.88 ± 0.31	7.49 ± 0.20	9.09 ± 0.32*†	8.63 ± 1.00*	↑ 1.6
PI	SFA	0.07 ± 0.01	0.10 ± 0.01*	0.10 ± 0.01*	0.06 ± 0.01*	ns
	MUFA	0.13 ± 0.01	0.29 ± 0.01*	0.44 ± 0.02*†	0.13 ± 0.02	↑
	PUFA	24.57 ± 0.28	26.00 ± 2.00	25.05 ± 1.68	24.79 ± 3.04	ns
	total PI	24.78 ± 0.28	26.40 ± 1.99	25.59 ± 1.68	24.98 ± 3.06	ns
LPE	SFA	1.52 ± 0.25	2.14 ± 0.08*	2.45 ± 0.11*†	1.25 ± 0.17	↑
	MUFA	0.18 ± 0.039	0.21 ± 0.012	0.28 ± 0.012*†	0.18 ± 0.03	↑
	PUFA	0.12 ± 0.023	0.14 ± 0.012	0.18 ± 0.013*†	0.12 ± 0.017	↑
	Total LPE	1.82 ± 0.30	2.49 ± 0.10	2.91 ± 0.12*†	1.55 ± 0.21	↑ 0.4

<sup>a</sup> Fatty acids were measured by ESI-MS/MS. Mouse hepatocytes were treated with 300 μM palmitate (Pal) with or without 60 μM UDCA-LPE for 20 h. All groups contained 0.5% BSA and 0.1% ethanol. Data were mean ± SD, N=4. All values were reported in nmol/mg protein. Significant difference: \*,  $p < 0.05$ , con versus Pal, Pal+UDCA-LPE or UDCA-LPE; †,  $p < 0.05$ , Pal versus Pal+UDCA-LPE. ns means not significant.

<sup>b</sup> Phospholipid (PL) class: PC, phosphatidylcholine; PE, phosphatidylethanolamine; PS, phosphatidylserine; PI, phosphatidylinositol; LPE, lysophosphatidylcholine. Fatty acid saturation: SFA, saturated fatty acids; MUFA, monounsaturated fatty acids; PUFA, polyunsaturated fatty acids.

Table 3 Molecular species of phospholipid fatty acids during lipoapoptosis and protection by UDCA-LPE<sup>a</sup>.

PL class	# carbon and double bonds <sup>b</sup>	con	Pal	Pal +UDCA-LPE	UDCA-LPE	Changes Pal+UDCA-LPE vs. Pal	PL species <sup>c</sup>
PC	PC 30:0	0.13 ± 0.01	0.24 ± 0.01*	0.20 ± 0.00*†	0.09 ± 0.01*	↓	14:0,16:0
	PC 32:2	0.08 ± 0.00	0.12 ± 0.0001*	0.14 ± 0.01*†	0.05 ± 0.01*	↓	16:1,16:1; 14:0,18:2
	PC 32:0	1.17 ± 0.05	5.92 ± 0.22*	4.63 ± 0.11*†	0.67 ± 0.08*	↓	16:0,16:0
	PC O 34:2	0.09 ± 0.00	0.11 ± 0.0001*	0.13 ± 0.00*†	0.07 ± 0.01*	↑	16:1,18:1; 16:0,18:2
	PC O 34:1	0.20 ± 0.01	0.24 ± 0.01*	0.26 ± 0.01*	0.13 ± 0.02*	ns	16:0,18:1; 18:0;16:1
	PC O 34:0	0.05 ± 0.00	0.10 ± 0.0001*	0.09 ± 0.00*†	0.03 ± 0.00*	↓	16:0,18:0
	PC 34:3	0.53 ± 0.01	0.68 ± 0.02*	0.79 ± 0.01*†	0.38 ± 0.05*	↑	16:0,18:3; 16:1,18:2
	PC 34:2	12.53 ± 0.27	14.28 ± 0.57*	15.64 ± 0.67*	8.99 ± 1.35*	ns	16:1,18:1; 16:0,18:2
	PC 34:1	9.06 ± 0.25	11.23 ± 0.32*	14.00 ± 0.48*†	7.79 ± 1.05*	↑	16:0,18:1; 18:0;16:1
	PC 34:0	0.30 ± 0.02	0.39 ± 0.02*	0.27 ± 0.01†	0.15 ± 0.03*	↓	16:0,18:0
	PC O 36:5	0.03 ± 0.00	0.03 ± 0.0001	0.04 ± 0.01*†	0.02 ± 0.004	↑	16:1,20:4; 16:0,20:5
	PC O 36:4	0.05 ± 0.00	0.05 ± 0.0001	0.06 ± 0.00*†	0.04 ± 0.007*	↑	18:1,18:3; 16:0,20:4
	PC O 36:2	0.43 ± 0.02	0.46 ± 0.01*	0.5 ± 0.02*	0.27 ± 0.04*	ns	18:0,18:2; 18:1,18:1
	PC 36:5	0.29 ± 0.02	0.34 ± 0.01*	0.42 ± 0.01	0.25 ± 0.04	↑	16:1,20:4; 16:0,20:5
	PC 36:2	5.07 ± 0.09	5.31 ± 0.18	6.05 ± 0.26*†	4.17 ± 0.58*	↑	18:1,18:1; 18:0,18:2
	PC 36:1	1.27 ± 0.05	1.27 ± 0.03	1.48 ± 0.07*†	1.22 ± 0.17	↑	18:0,18:1; 16:0,20:1
	PC 38:6	4.53 ± 0.20	5.63 ± 0.28*	6.20 ± 0.27*	4.96 ± 0.72	ns	16:1,22:5; 16:0,22:6
	PC 38:5	1.04 ± 0.05	1.19 ± 0.05*	1.46 ± 0.04*†	1.13 ± 0.17	↑	18:1,20:4; 16:0,22:5
PC 40:5	0.29 ± 0.01	0.32 ± 0.01*	0.39 ± 0.02*†	0.31 ± 0.04	↑	18:0,22:5	
PE	PE 32:2	0.01 ± 0.00	0.03 ± 0.0001*	0.03 ± 0.00*†	0.004 ± 0.0001*	↓	16:1,16:1; 14:0,18:2
	PE 32:1	0.04 ± 0.00	0.57 ± 0.02*	0.37 ± 0.01*†	0.02 ± 0.005*	↓	14:0,18:1; 16:0,16:1
	PE 32:0	0.05 ± 0.00	1.10 ± 0.02*	0.72 ± 0.02*†	0.03 ± 0.003	↓	16:0,16:0
	PE 34:2	0.84 ± 0.02	1.37 ± 0.05*	1.54 ± 0.04*†	0.61 ± 0.10*	↑	16:1,18:1; 16:0,18:2
	PE 34:1	0.23 ± 0.01	0.78 ± 0.01*	1.00 ± 0.03*†	0.20 ± 0.02	↑	16:0,18:1; 18:0;16:1
	PE 34:0	0.10 ± 0.01	0.70 ± 0.04*	0.39 ± 0.02*†	0.07 ± 0.01	↓	16:0,18:0
	PE 36:3	0.42 ± 0.02	0.47 ± 0.02	0.58 ± 0.03*†	0.42 ± 0.07	↑	18:1,18:2; 18:0,18:3
	PE 36:1	0.16 ± 0.00	0.15 ± 0.01	0.19 ± 0.01†	0.18 ± 0.04	↑	18:0,18:1; 16:0,20:1
	PE 38:6	3.31 ± 0.13	4.69 ± 0.22*	5.22 ± 0.24*	3.46 ± 0.50	ns	16:1,22:5; 16:0,22:6;18:1,20:4
PS	PS 38:6	0.20 ± 0.01	0.33 ± 0.02*	0.42 ± 0.03*†	0.35 ± 0.03*	↑	16:1,22:5;16:0,22:6;18:1,20:4
	PS 38:5	0.07 ± 0.01	0.09 ± 0.01*	0.12 ± 0.01*†	0.07 ± 0.01	↑	18:1,20:4; 16:0,22:5
	PS 38:4	1.38 ± 0.03	1.27 ± 0.05	1.43 ± 0.06	1.60 ± 0.19*	ns	18:0,20:4
	PS 40:6	2.58 ± 0.14	3.20 ± 0.16*	4.32 ± 0.14*†	4.11 ± 0.55*	↑	18:1,22:5; 18:0,22:6
	PS 40:5	0.21 ± 0.04	0.22 ± 0.02	0.33 ± 0.03*†	0.19 ± 0.03	↑	18:0,22:5
	PS 42:6	0.00 ± 0.00	0.02 ± 0.0001	0.08 ± 0.01*†	0.06 ± 0.04*	↑	18:1,24:5; 18:0,24:6
PI	PI 34:1	0.05 ± 0.00	0.17 ± 0.01*	0.22 ± 0.02*†	0.05 ± 0.01	↑	16:0,18:1; 18:0;16:1
	PI 36:1	0.08 ± 0.02	0.13 ± 0.01	0.23 ± 0.02*	0.08 ± 0.01*	ns	18:0,18:1; 16:0,20:1
	PI 38:5	0.98 ± 0.03	1.04 ± 0.1	1.20 ± 0.08*	1.33 ± 0.18*	ns	18:1,20:4; 16:0,22:5
LPE	LPE 16:0	0.46 ± 0.07	0.72 ± 0.02*	0.79 ± 0.03*†	0.31 ± 0.05*	↑	
	LPE 18:2	0.04 ± 0.007	0.048 ± 0.005	0.06 ± 0.007*†	0.04 ± 0.007	↑	
	LPE 18:1	0.18 ± 0.034	0.18 ± 0.01	0.24 ± 0.009*†	0.17 ± 0.04	↑	
	LPE 18:0	0.97 ± 0.17	1.33 ± 0.06*	1.6 ± 0.07*†	0.85 ± 0.12	↑	
	LPE 20:4	0.07 ± 0.009	0.08 ± 0.006	0.09 ± 0.007*†	0.08 ± 0.01	↑	
	LPE 20:0	0.05 ± 0.01	0.05 ± 0.001	0.06 ± 0.004*†	0.04 ± 0.004	↑	

<sup>a</sup> Same treatment as Table 2; data in nmol/mg protein were mean ± SD, N=4. Significant difference: \*, *p*<0.05, con versus Pal, Pal+UDCA-LPE or UDCA-LPE; †, *p*<0.05, Pal versus Pal+UDCA-LPE. ns means not significant.

<sup>b</sup> Species annotation is based on the assumption that only even acyl chains are present.

<sup>c</sup> The fatty acid combination are based on the fatty acids detected by GC-MS (compare with Table 1).

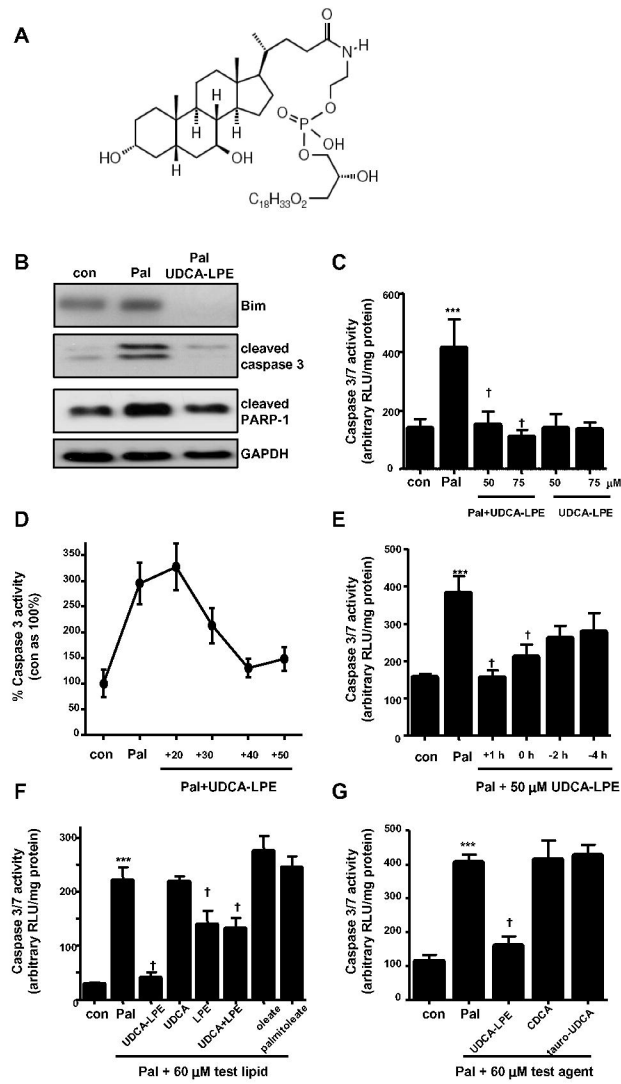


**Figure 1**

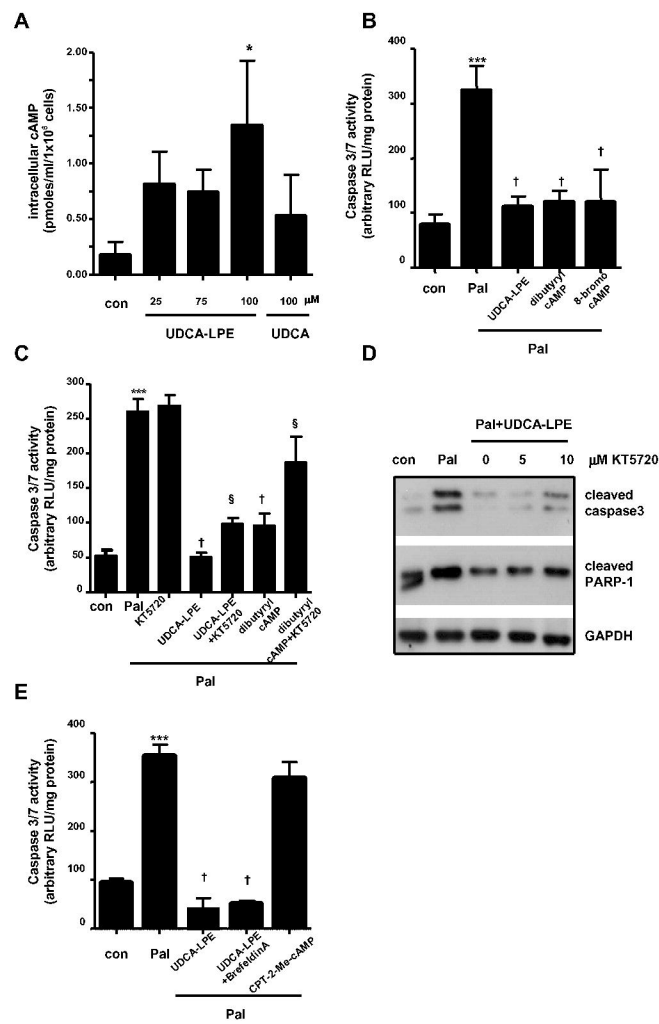


Figure 2

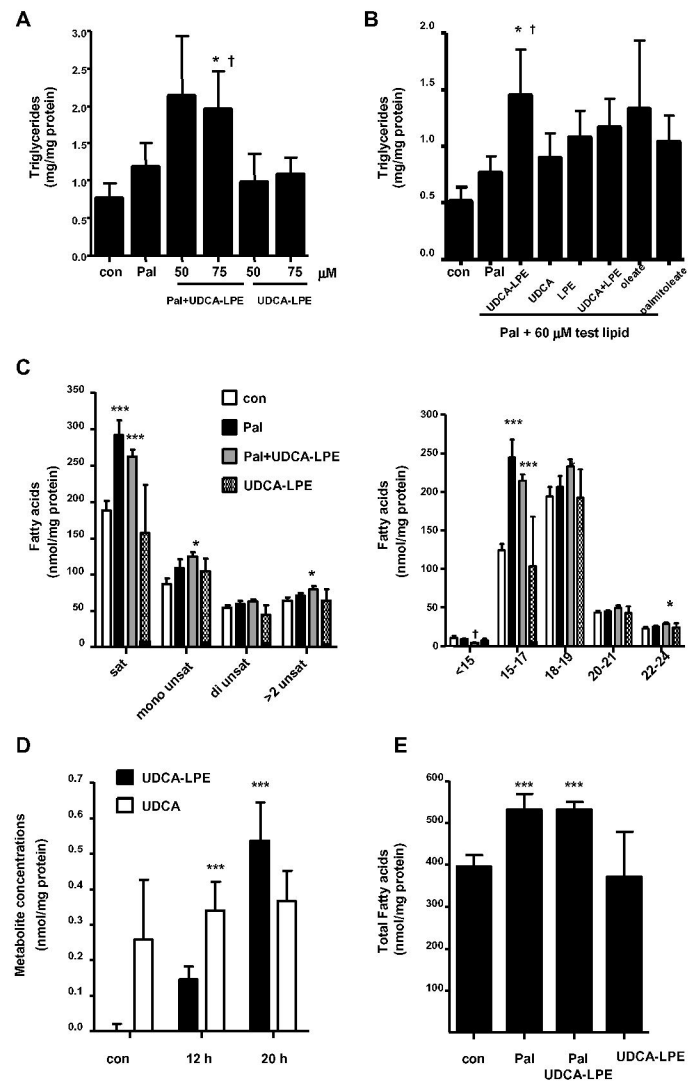


Figure 3

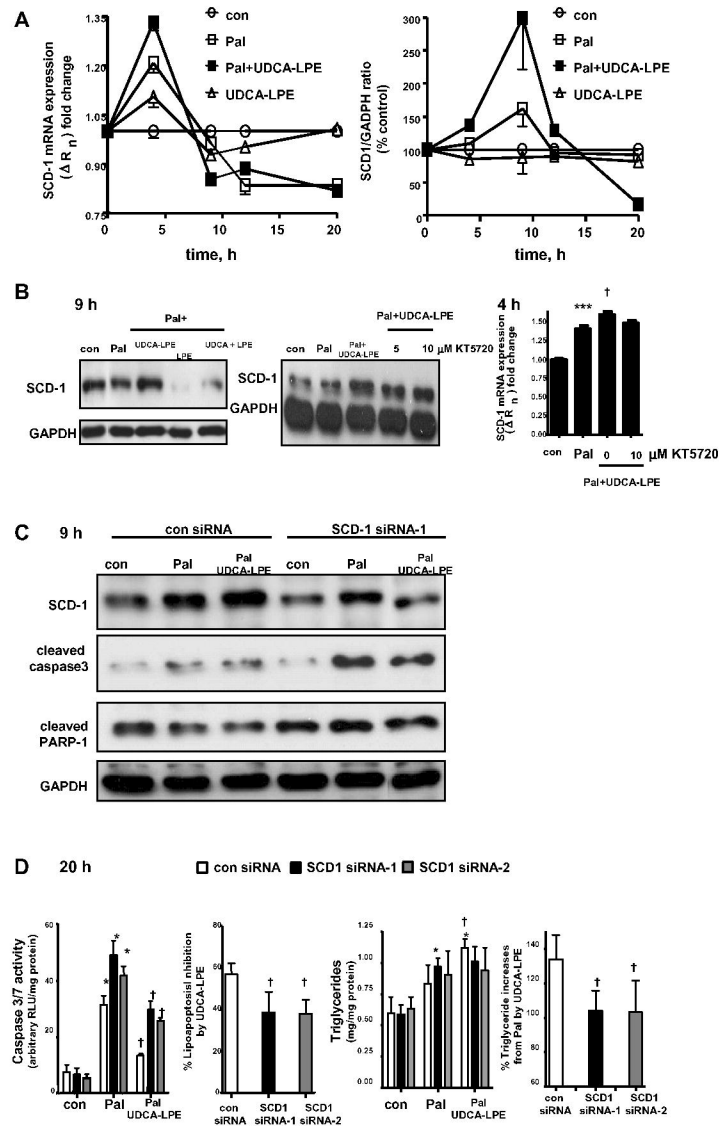


Figure 4

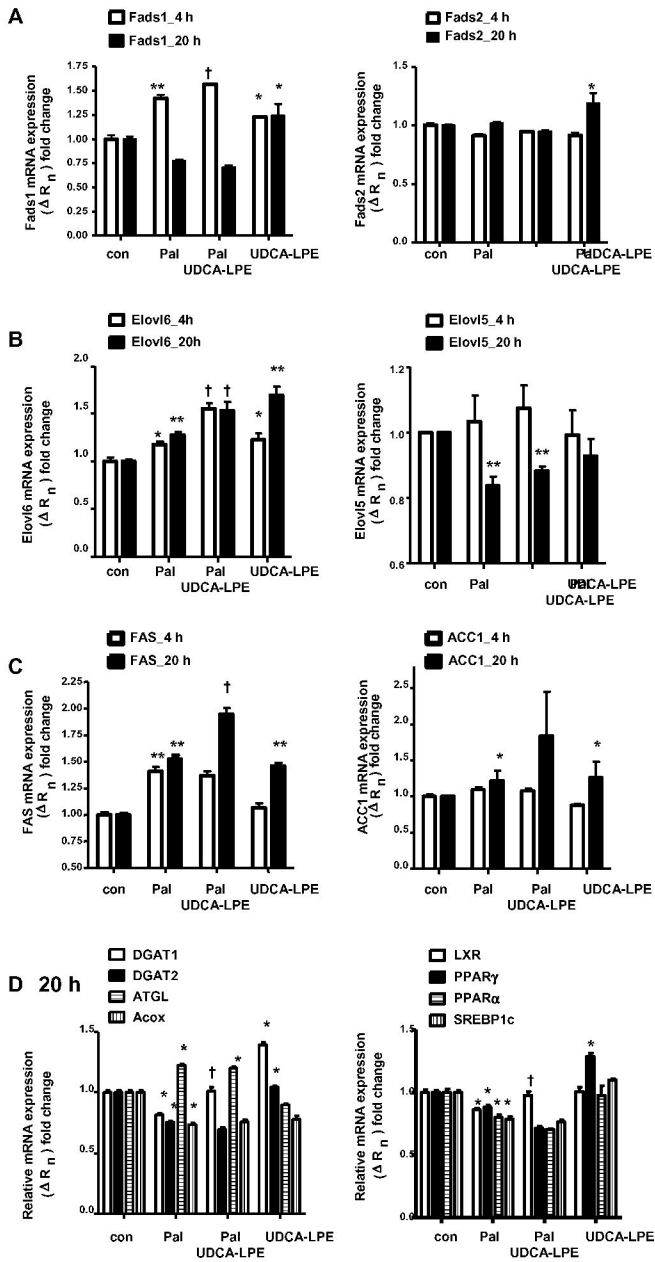


Figure 5



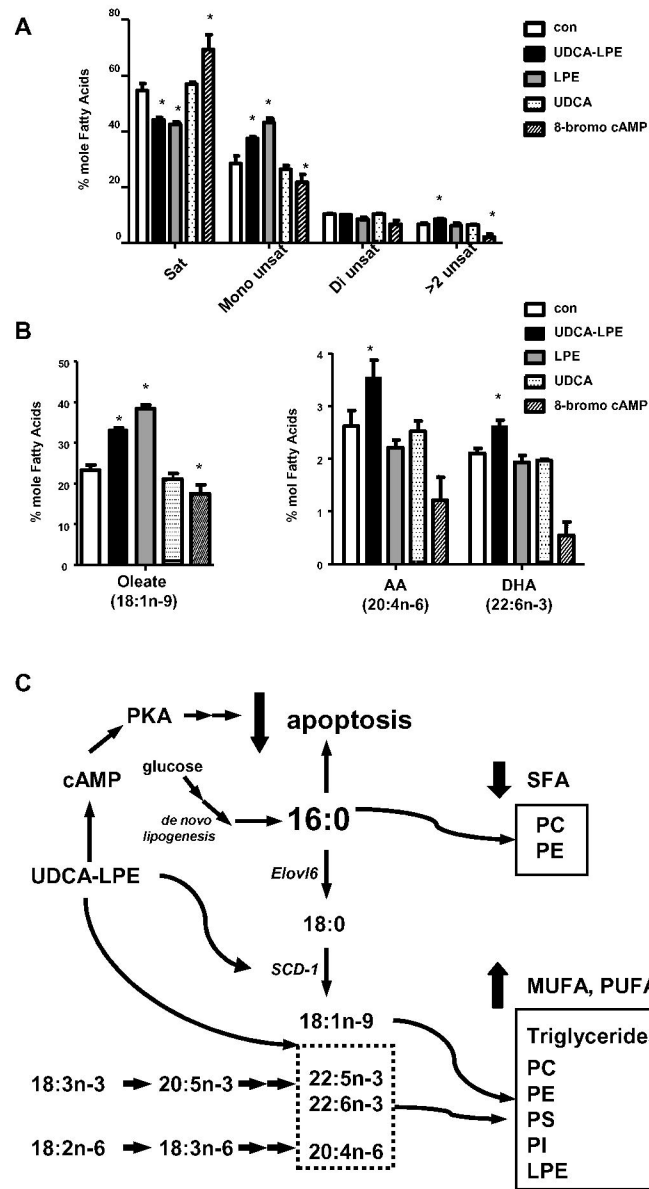


Figure 6